[Frontiers in Bioscience 14, 2944-2958, January 1, 2009]

The dark and the bright side of Stat3: proto-oncogene and tumor-suppressor

Andrea Ecker[1], Olivia Simma[2], Andrea Hoelbl[2], Lukas Kenner[3,4], Hartmut Beug[1], Richard Moriggl[3], Veronika Sexl[2]

[1]Institute of Molecular Pathology (IMP), Austria, [2]Institute of Pharmacology, Medical University of Vienna (MUW), Austria,[3]Ludwig-Boltzmann-Institute for Cancer Research (LBI-CR), Austria, [4]Institute of Clinical Pathology, Medical University of Vienna (MUW), Austria

TABLE OF CONTENTS

1. ABSTRACT

Stat transcription factors have been implicated in tumorigenesis in mice and men. Stat3 and Stat5 are considered powerful proto-oncogenes, whereas Stat1 has been demonstrated to suppress tumor formation. We demonstrate here for the first time that a constitutive active version of Stat3alpha (Stat3alphaC) may also suppress transformation. Mouse embryonic fibroblasts (MEFs) deficient for p53 can be transformed with either c-myc or with rasV12 alone. Interestingly, transformation by c-myc is efficiently suppressed by co-expression of Stat3alphaC, but Stat3alphaC does not interfere with transformation by the rasV12-oncogene. In contrast, transplantation of bone marrow cells expressing Stat3alphaC induces the formation of a highly aggressive T cell leukemia in mice. The leukemic cells invaded multiple organs including lung, heart, salivary glands, liver and kidney. Interestingly, transplanted mice developed a similar leukemia when the bone marrow cells were transduced with Stat3beta, which is also constitutively active when expressed at significant levels. Our experiments demonstrate that Stat3 has both – tumor suppressing and tumor promoting properties.

2. INTRODUCTION

The Jak-Stat pathway transmits cytokine and growth factor signals into the nucleus of target cells to control gene expression. Jak-Stat activation is important for many normal cellular functions but aberrant activity is associated with tumorigenesis. Stat proteins are activated by tyrosine kinase signaling which determines their dimerization and nuclear translocation, DNA binding and activation of target gene expression (1-3).

Although Stats have been originally described in the context of physiological processes, an increasing number of recent studies have implicated Stat activation in transformation and tumor progression. In particular constitutively active Stat5 and Stat3 have been detected in human as well as murine tumors. The generation of a constitutively active mutant of Stat3 (Stat3alphaC) allowed for the first time to directly link Stat3 to tumor formation and defined Stat3 as a proto-oncogene (4). The expression of Stat3alphaC in a rat fibroblast cell line transformed the cells and induced tumor formation in nude mice (4). The generation of gene targeted mice allowed further insights

into the function of Stat3 and established Stat3 as an important tumor promoter (5, 6).
So far, no mutations of Stat3 have been detected in human patients suffering from cancer, Stat3 activation is the result of persistent stimulation via upstream signals. Stat3 has been shown to be activated by several different oncogenes such as v-src or v-abl. In addition, many growth factor receptors that are implicated in tumorigenesis like the epidermal growth factor receptor, vascular endothelial growth factor receptor or human epidermal growth factor receptor 2 activate Stat3. The knock down of Stat3 by siRNA or using dominant negative versions in human cancer cells has proven the importance of Stat3 signaling in tumor progression and maintenance. Stat3 is now considered a potential future drug target (7-9).

The target genes regulated by Stat3 supporting oncogenesis can be grouped according to their function (9). One group comprises anti-apoptotic target genes as bcl_{xL}, mcl-1 or survivin that enhance the survival of transformed cells (10). Other target genes that regulate proliferation include D type cyclins and c-myc and link elevated Stat3 activation to accelerated cell cycle progression (11). Besides these Stat3-mediated effects that are visible *in vitro* further important consequences of Stat3 activation for tumor progression can only be analyzed *in vivo*. This includes Stat3 target genes such as vascular endothelial growth factor, hepatocyte growth factor, basic fibroblast growth factor and hypoxia inducible factor 1alpha, all important mediators of angiogenesis. Furthermore, Stat3 activation provides a direct link to immuno-suppression. Recent work has elucidated that the inhibition of Stat3 in tumor cells significantly enhances the immunological response against the growing tumor. Several mechanisms seem to account for the Stat3 mediated immune-suppression, among them effects on the maturation and presentation of dendritic cells (12). One explanation for the diversity of responses and the functional heterogeneity evoked by Stat3 is the fact that two differentially spliced isoforms of Stat3 exist, Stat3alpha and Stat3beta. Stat3beta has a shorter and unique transcriptional activation domain at the C-terminus. It has been initially viewed as having antagonistic functions being dominant negative. Only recently, it was proven that both, Stat3alpha and Stat3beta have unique and specific functions and might modulate their own sets of target genes (13).

In this study we show that the definition of functional heterogeneity of Stat3 reaches even further complexity. Dependent on the cellular context Stat3 may act as a tumor suppressor or as a tumor promoter. In primary fibroblasts the tumor suppressing activities of Stat3 dominate. In contrast, in primary hematopoietic cells both Stat3 isoforms act as tumor promoter.

3. MATERIALS AND METHODS

3.1. [^{3}H] thymidine incorporation

Cells were plated at a density of $2x10^5$ cells in 96 round bottom wells. 0.1 microCi [^{3}H]thymidine/well was added 18 hours after plating for another 12 hours.

3.2. Retroviral constructs

For retroviral infections the following inserts were cloned into a pMSCV-IRES-eGFP backbone: Stat3alpha, Stat3alphaC, Stat3beta and Stat3betaC. The point-mutations causing constitutive activation of Stat3 are described in (4).

3.3. Tissue culture and retroviral infections of fibroblasts

The human embryonic kidney cell line 293T, the retroviral producer cell line Phoenix, the murine embryonic cell line NIH3T3 and $Stat3^{-/-}$ mouse embryonic fibroblasts (MEFs) were grown in DMEM (HEPES modification, Sigma) supplemented with 10% fetal bovine serum (FCS, Gibco, BRL), penicilline (1 U/ml)/ streptomycine (100 microg/ml) (Biochrom AG) and 2 mM L-glutamine (GIBCO BRL). Cells were grown at humidified 37° C, 5% CO_2. For retroviral infections of fibroblasts, supernatant of Phoenix cells, transiently infected with pMSCV-IRES-eGFP constructs using Lipofectamine Plus (Invitrogen Life Technologies), was transferred to the target cells for 12 hours.

3.4. Retroviral infection and bone marrow transplantation studies

Bone marrow transplantation studies were performed as described previously (14, 15). Briefly, stable producer cell lines (GP+E86) were seeded onto gelatine-coated dishes, grown to confluency and subsequently irradiated (1,400 RADs). Bone marrow from 8-12 week old male C57/Bl6 X 129/Sv F1 mice was co-cultivated with the producer cell lines in DMEM supplemented with 10% FCS, 1x penicillin/streptomycin, 2 mM L-glutamine, 1x MEM non essential amino acids, 1 mM MEM sodium pyruvate, 10 mM Hepes pH 7.3, 50 ng/ml mIL-6 (R&D systems), 20 ng/ml recombinant mIL-3 (PrepCo Tech Inc), 500 ng/ml mSCF (R&D systems) and 6 microg/ml polybrene at a concentration of $2.25x10^6$ cells/ml. After 60 hours, $5x10^6$ infected bone marrow cells were injected into the tail vein of lethally irradiated (1,080 RADs) female C57/Bl6 X 129/Sv F1 mice. Mice were every other day watched for signs of disease and sick mice were sacrificed for the analysis of bone marrow, spleen and liver infiltration.

3.5. Western Blot analysis

For Western blot analysis, cells were rinsed twice in icecold PBS, scraped off and lysed in whole cell extract buffer containing protease and phosphatase inhibitors (20 mM Hepes, pH 7.9, 20% glycerol, 50 mM KCl, 1 mM EDTA, 1 mM DTT (Sigma), 400 mM NaCl, 5 microg/ml leupeptin (Boehringer Mannheim), 0.2 U/ml aprotinin (Bayer), 1mM PMSF (Boehringer Mannheim), 5 mM Na_3VO_4, 10 mM NaF, 5 mM beta-glycerophosphate). Protein concentrations were determined by a Bradford assay (Bio-Rad). Protein extracts (10-20 microg) were then separated on a 7.5% SDS polyacrylamide gel and transferred onto NitroPure membranes (Osmonics) by semi-dry blotting. Subsequently, membranes were probed with antibodies against Stat3 (K15), c-Jun (H-79), JunB (210), p16 (M-156), cdk6 (C-21), cyclin D1 (178) and cyclin D2 (593), all purchased from Santa Cruz Biotechnology and beta-actin (Ac-54, Sigma).

3.6. Fibroblast focus formation assays

Once retrovirally infected, cells were grown to complete confluency and then no more passaged until foci formation became apparent. Plates were then washed twice in PBS, cells were fixed in 10% formaldehyde/PBS for 30 minutes and then stained with 4% Giemsa (Fluka)/PBS for two hours.

3.7. Colony formation assay in growth-factor free methylcellulose

MEFs deficient for p53 were retrovirally infected with c-myc or co-infected with c-myc and Stat3alphaC and subsequently plated in cytokine-free methylcellulose at a density of $2{,}5x10^5$ cells/ml in 35 mm dishes. After 10 days, cloning efficiency was evaluated by counting colonies by light microscopy (Leica Fluovert microscope, 4x magnification). The assays were performed in triplicates. Cells retrovirally infected with the empty vector did not result in growth-factor independent colonies.

3.8. Flow cytometric analysis (FACS)

Flow cytometric analysis was carried out using FACSCalibur (Becton Dickinson) and CellQuest software. Single cell suspensions were pre-incubated with CD16/CD32 antibodies (BD Biosciences) to prevent non-specific Fc-receptor-mediated binding. Subsequently, $5x10^5$ cells were stained with monoclonal antibodies conjugated with fluorescent markers. The following antibodies were used: CD8a (Ly1.2)-FITC, CD4 (L3T4)-APC, Thy1.2-PE (all Becton Dickinson).

3.9. Tumor formation in *nu/nu* mice

For analysis of tumor formation in vivo, 3x106 cells were injected subcutaneously into 6 weeks old nu/nu mice. Tumor size was measured 10 days after injection. These animal studies were carried out according to Austrian law. Animals were housed at the Biomedical Research Institute, Medical University of Vienna, under specific pathogen-free sterile conditions.

3.10. Gel shift assays (EMSAs)

293T cells or fibroblasts were either left un-stimulated or were stimulated with 20 ng/ml recombinant species specific mIL-6 (R&D systems) for 30 min at 37 °C. The cells were harvested and cell pellets were resuspended in whole cell extract buffer (see above). Oligos were annealed at high equimolar concentration in a 200 microl reaction in 0.0625X PCR buffer II (Roche), 0.94 mM $MgCl_2$ by heating up to 95 °C. Five picomol of double stranded annealed DNA were labeled for 1 hour at 37 °C with 5 microl gamma-ATP ^{32}P (10000-30000 cpm/microl) using polynucleotide kinase (10 units, Roche) and then purified on size exclusion columns (Micro Bio-Spin 6 chromatography columns, Bio-rad). Whole cell extracts were incubated with labeled probe (20 microl reaction: 20 microg protein extract, 1 microl probe (8000 cpm/fmol), 4 microl 5x binding buffer (50 mM Tris, 5 mM DTT, 1 mM PMSF, 0.5 mM EDTA, 25% glycerol, 250 mM NaCl, 0.5% NP4O), 2 microg Poly dI-dC, 20 microg BSA) for 5-15 min at RT and for supershift with 1 microl of antibody for 5 min on ice. Complexes were separated on non-denaturing 4% acrylamide 0.25x TBE gels, transferred onto filter paper (Whatman chromatography paper), dried and exposed to films.

3.11. Reverse transcription polymerase chain reaction (RT-PCR) and analysis of sex-determining region (SRY) expression

First-strand cDNA synthesis and PCR amplification were performed using a RT-PCR-kit (GeneAmp RNA PCR kit; Applied Biosystems) according to manufacturer´s instructions. To avoid genomic contamination RNA was DNase I treated (Roche Applied Science) and the RNA samples were thereafter subjected to an RT-PCR that did not give a PCR product and hence verified the absence of any contaminations. Primer pairs were designed for the detection of pMSCV-Stat3 constructs by RT-PCR with one oligo lying in the retroviral backbone and one primer within the Stat3 insert. The specificity of the primers was controlled for using several leukemic cell lines that express either pMSCV- IRES-GFP, pMSCV-Stat-5-IRES-GFP or pMSCV-cdk6-IRES-GPF (data not shown). The following primer pairs were used: N-terminus: pMSCVfw: gcc ctc act cct tct cta gg, stat3rev: ctg gca cct tgg att gag agt; alpha C-terminus: stat3alphafw: gca gtt tgg aaa taa cgg tga agg tgc, pMSCVrev: tat tcc aag cgg ctt cgg cca gta a; beta C-terminus: stat3betafw: gtg aca cca ttc att gat gca gtt tgg, pMSCVrev: tat tcc aag cgg ctt cgg cca gta a; reactions were performed using AmpliTaq Gold Polymerase (Roche Molecular Systems). RT-PCR for beta-actin served as control: beta-actin: betaactfw: act cct atg tgg gtg acg ag, betaactrev: cag gtc cag acg cag gat ggc. The male SRY specific cDNA was amplified as described previously (16).

3.12. Mouse pathology, histology and immunohistochemistry

Tissues were fixed in 4% formaldehyde/PBS, paraffin-embedded, sectioned, and stained with hematoxylin-eosin (H&E). Immunohistochemistry was performed on serial sections prepared from paraffin-embedded, formalin-fixed organ sections using the indirect immunoperoxidase staining technique. Endogenous peroxidase was blocked by methanol/H_2O_2. Prior to staining with antibodies, sections were pretreated by microwaving. Sections were stained with anti-CD3 (DAKO), anti-FasR and anti-FasL (Dianova) diluted in 0.05 M Tris-buffered saline (TBS, pH 7.5) plus 1% BSA. Then slides were washed and incubated with biotinylated goat anti-mouse IgG for 30 minutes, washed, and exposed to biotin-peroxidase complex. AEC (red) or DAB (brown) were used as chromogen. Slides were counterstained in Mayer´s Hemalaun. Tissue sections were also stained with hematoxylin and eosin. Histopathology analysis was performed with paraffin-embedded specimens. To compare the expression levels of FasL from normal lung tissue and diseased animals, Stat3alphaC and Stat3beta, target protein expression analysis was performed using immunofluorescence microscopy and digital image analysis techniques. The *in vivo* protein expression of FasL was measured with the image analysis software of TissueQuest™ from TissueGnostics. The background staining was defined using normal lung tissue that was negative for FasL. The thus derived staining was subtracted

from the tumor samples and the results are depicted as mean intensity.

3.13. Statistical analysis

Statistics were carried out using a paired t-test or a one-way ANOVA followed by a Tukey test as appropriate.

4. RESULTS

4.1. Stat3alphaC expression blocks cell proliferation in murine fibroblasts

The effects of Stat3alphaC expression on the growth of murine fibroblasts were first tested in a widely established model system, in immortalized NIH3T3 cells. Cell proliferation was monitored by comparing vector-infected cells to Stat3alphaC expressing cells. As depicted in Figure 1A, Stat3alphaC decreased cell proliferation when analyzed by [^{3}H]thymidine incorporation assays. To screen for a transforming ability of Stat3alphaC the infected as well as the control cells were plated on gelatine-coated dishes and maintained without further splitting. No foci formation was observed after a three weeks period indicating that the Stat3alphaC infected cells had not lost contact-inhibition (Figure 1B). Also cloning Stat3alphaC in the originally described vector back bone (RcCMV-Stat3alphaC) did not change our results. Again, we failed to see any spontaneous focus formation (data not shown). Several proteins are associated with growth inhibition in murine fibroblast, among them JunB – a known target gene of Stat3 and an important tumor suppressor protein (17). As depicted in Figure 1C, we found that the expression of Stat3alphaC indeed up-regulated the AP-1 transcription factor JunB and the cell cycle inhibitor protein $p16^{INK4a}$. Whereas cyclin D1 was only slightly up-regulated, we observed a significant down-regulation of the cell cycle kinase cdk6, which has been described to be controlled by JunB (18). No increase in apoptotic cell death was observed upon Stat3alphaC infection; accordingly we failed to detect any difference in the expression of bcl_{xL} and survivin (data not shown). Taken together, we conclude that the enforced expression of Stat3alphaC in murine fibroblasts resulted in a reduction of cell proliferation rather than promoting transformation.

4.2. Stat3alphaC blocks c-myc induced transformation in primary murine fibroblasts

JunB is not only a known inhibitor of cell proliferation in murine fibroblasts but also capable of inhibiting transformation. We therefore established an assay system that allowed us to study whether Stat3alphaC would influence transformation by a single oncogene. MEFs from $p53^{-/-}$ mice were prepared; $p53^{-/-}$ MEFs allow transformation by a single oncogene e.g. by either c-myc or a constitutive active mutant of ras (rasV12) alone. Figure 2A summarizes our efforts. Infection of $p53^{-/-}$ MEFs with either rasV12 or c-myc resulted in loss of contact inhibition and focus formation. Most interestingly, focus formation by c-myc - but not rasV12 - was blocked by co-infection and the concomitant expression of Stat3alphaC. To repeat and verify this surprising result with a different assay system, the following experiment was performed: $p53^{-/-}$ MEFS were infected with c-myc in combination with an empty vector or Stat3alphaC and subsequently plated in growth factor-free methylcellulose (Figure 2B-D). As an additional control for the infection process, western blots were performed (Figure 2C). The cells were subsequently cloned in growth factor free methyl cellulose to test for anchorage independent growth. The colonies were counted after ten days. The c-myc-infected cells gave rise to significantly higher colony numbers when co-infected with the empty vector compared to co-infection with Stat3alphaC (Figure 2D). To test tumor formation *in vivo* we injected an aliquot of the infected cells subcutaneously into *nu/nu* mice. Ten days thereafter solid tumors were excised. Tumors were detected in all mice that had been injected with fibroblasts infected with either rasv12 or c-myc alone or rasv12 in combination with Stat3alphaC. No tumor formation could be detected when c-myc was co-expressed with Stat3alphaC (Figure 2E). Moreover, we used bcl_{xL} to evoke spontaneous transformation in $p53^{-/-}$ MEFs that was readily detectable in focus formation assays. Again, co-infection with Stat3alphaC abolished focus formation indicating that Stat3alphaC not only blocked oncogene-induced but also spontaneous transformation (Figure 2F).

4.3. Stat3beta is constitutively active when expressed in fibroblasts

Our data so far indicated that Stat3alphaC was rather acting as a tumor suppressor than promoting tumor formation. However, transformation is a process that strongly depends on the cellular context. We therefore decided to express constitutive active versions of Stat3 in a different setting involving primary cells and to include both - Stat3alpha and Stat3beta - that had been shown to have unique and non-overlapping functions. Analogous to Stat3alphaC an active version of Stat3beta was generated, where constitutive dimer formation was induced by the same mutation in the SH2 domain (in the following termed Stat3betaC). All retroviral constructs were cloned into a pMSCV-IRES-GFP backbone and tested by transient infections into 293T cells. As expected, the transfection of 293T cells with Stat3alphaC resulted in constitutive Stat3 DNA binding activity that was further enhanced by IL-6 treatment. The expression of wild type Stat3alpha resulted in a Stat3 DNA binding activity solely in the presence of IL-6. Most interestingly, Stat3beta constitutively bound DNA in our assay conditions irrespective whether the activating mutation was present or not. Super-shift experiments verified that the DNA binding was indeed caused by a Stat3 complex (Figure 3A). Since the antibody recognizes the C-terminus, only Stat3alpha is supershifted. Western blot analysis revealed that the constitutive DNA binding of Stat3beta in the absence of IL-6 was accompanied by constitutive tyrosine phosphorylation (data not shown). As Stat3beta lacks the serine phosphorylation site, serine phosphorylation was only detectable on Stat3alpha (data not shown) To investigate whether the persistent activation of Stat3beta is a distinct property of 293T cells and requires the presence of wild type Stat3, the experiments were repeated in $Stat3^{-/-}$ fibroblasts. Comparable results were obtained (Figure 3B). Again, the enforced expression of Stat3beta induced Stat3 DNA binding activity that was paralleled by tyrosine

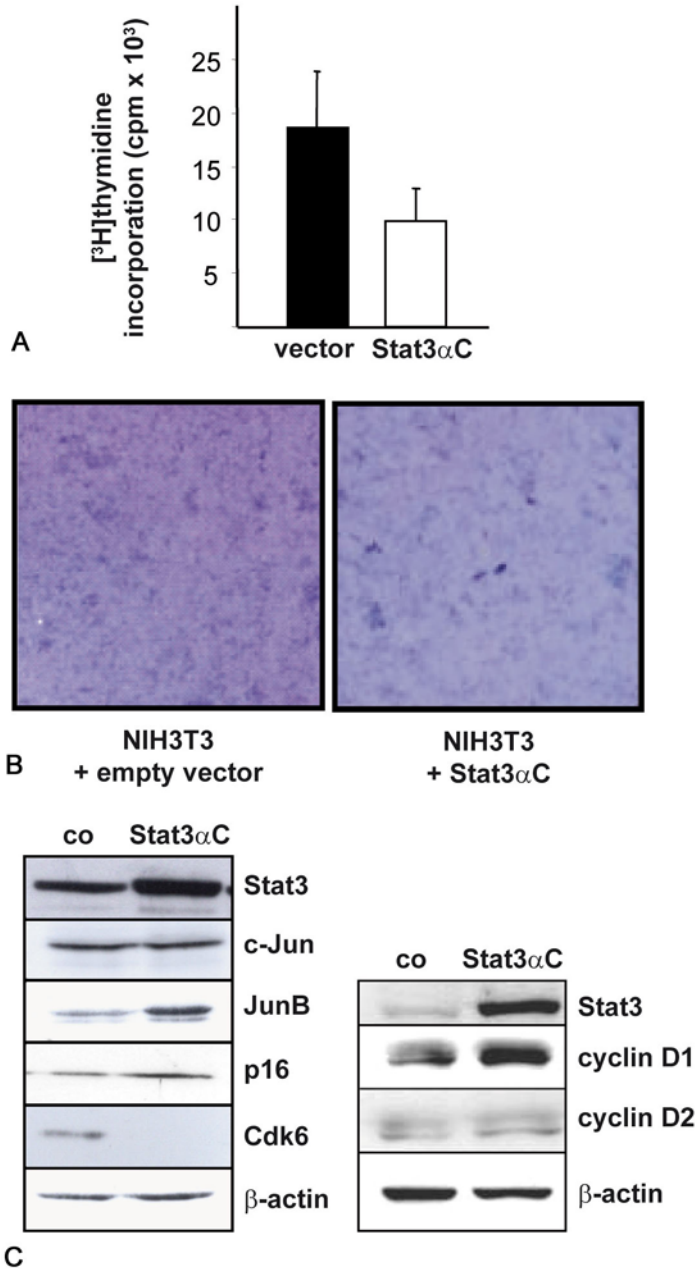

Figure 1. Cell cycle progression is decreased by the expression of Stat3alphaC in NIH3T3 cells. (A) NIH3T3 cells were infected with either Stat3alphaC or an empty vector and [^{3}H] thymidine incorporation assays were performed. (B) In a long-term culture assay, NIH3T3 cells expressing Stat3alphaC showed no increased loss of contact-dependence as compared to cells transfected with the empty vector. (C) For the analysis of expression levels of known Stat3 targets 20microg of protein lysate of NIH3T3 cells infected with Stat3alphaC or an empty vector were subjected to western blot analysis. Beta-actin expression was used as an internal control.

phosphorylation irrespective whether IL-6 was present or not (data not shown).

4.4. Constitutive active Stat3 (Stat3alphaC and Stat3beta) induces leukemia in mice

Stat3 affects hematopoiesis at various levels including B cell proliferation or granulopoiesis (19, 20). We therefore addressed the role of constitutive Stat3 isoforms in a bone marrow transplantation setting. For this experiment bone marrow was isolated and infected with Stat3alpha, Stat3alphaC, Stat3betaC or the empty vector alone. We abstained from including Stat3beta since no significant difference regarding activation was observed compared to Stat3betaC. However, in a later experiment Stat3beta was included and showed super-imposable results regarding disease-latency and phenotype to infections with

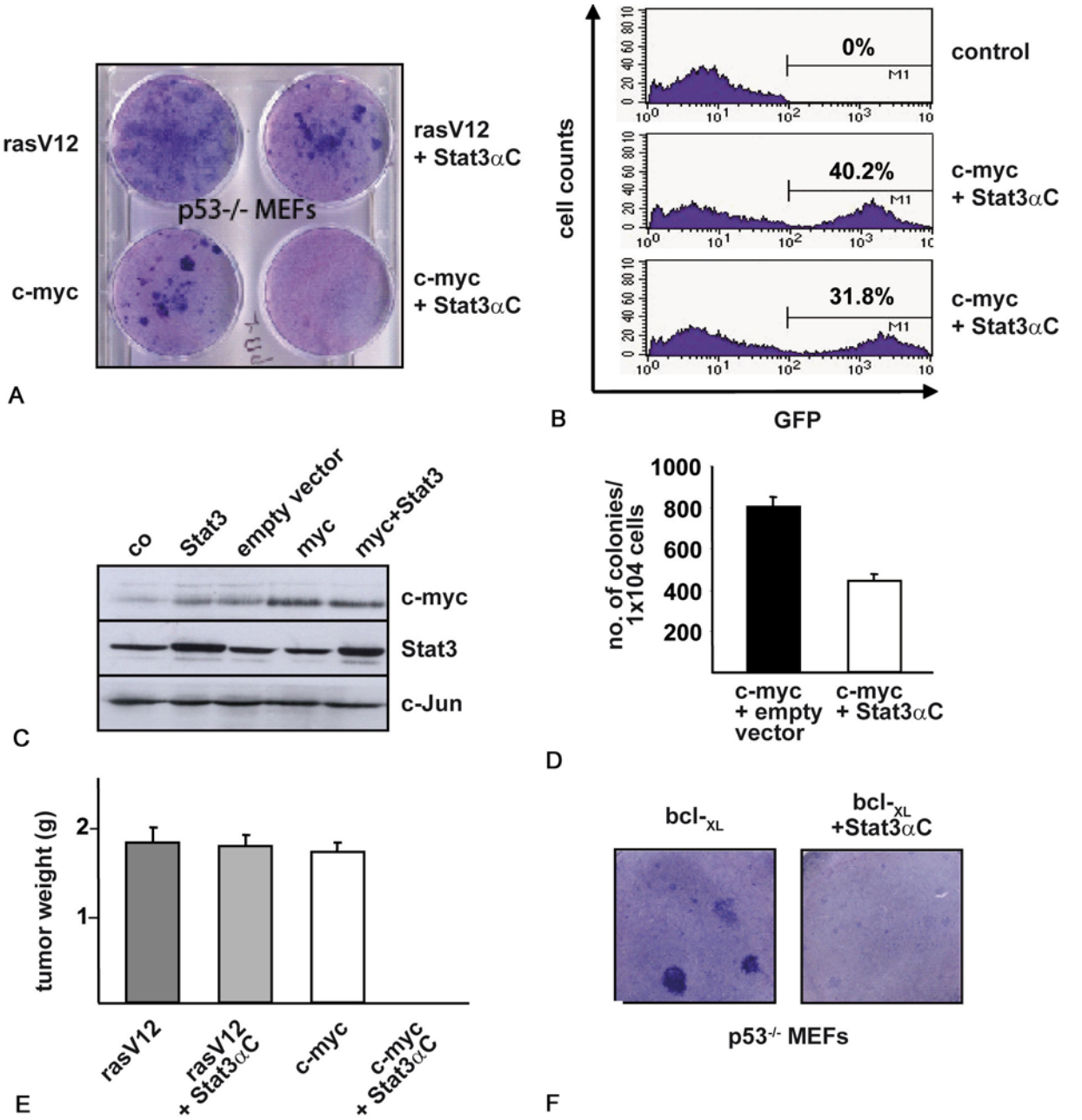

Figure 2. Stat3alphaC decreases the transformation capability of $p53^{-/-}$ MEFs *in vitro* and *in vivo*. (A) Focus formation assay of $p53^{-/-}$ MEFs. Cells were examined for loss of contact-dependence upon infection with a constitutively active mutant of ras (rasV12), c-myc or co-infection of each gene together with Stat3alphaC. Infection rates were as follows: 15.1% for rasV12, 7% for c-myc, 14.6% for rasV12+Stat3alphaC and 16.4% for c-myc + Stat3alphaC. Black areas (foci) indicate transformed proliferating cells with loss of contact-dependence. (B) - (D) Colony formation assay in growth-factor-free methylcellulose. $p53^{-/-}$ MEFs were retrovirally infected with c-myc alone or co-infected with c-myc and Stat3alphaC, analysed for GFP expression by flow cytometry (B) and subjected to western blot analysis to verify enhanced expression levels of Stat3 and c-myc in infected cells, whereas c-Jun was used as an internal control (C). Subsequently, cells were seeded in growth-factor-free methylcellulose and colonies were counted after 10 days. Data obtained from 3 individual experiments are summarized in a bar graph and represent means +/- SEM (D). (E) The capability of $p53^{-/-}$ MEFs expressing either rasV12, c-myc or rasV12 or c-myc together with Stat3alphaC to form tumors *in vivo* was examined by subcutaneous injection of $3x10^6$ cells into *nu/nu* mice. 10 days after transplantation tumor weights of diseased mice were measured and are summarized in a bar graph. Data represent means +/- SEM. (F) Spontaneous focus formation was also abolished in $p53^{-/-}$ MEFs co-transfected with bcl-$_{xL}$ and Stat3alphaC compared to cells expressing only bcl-$_{xL}$.

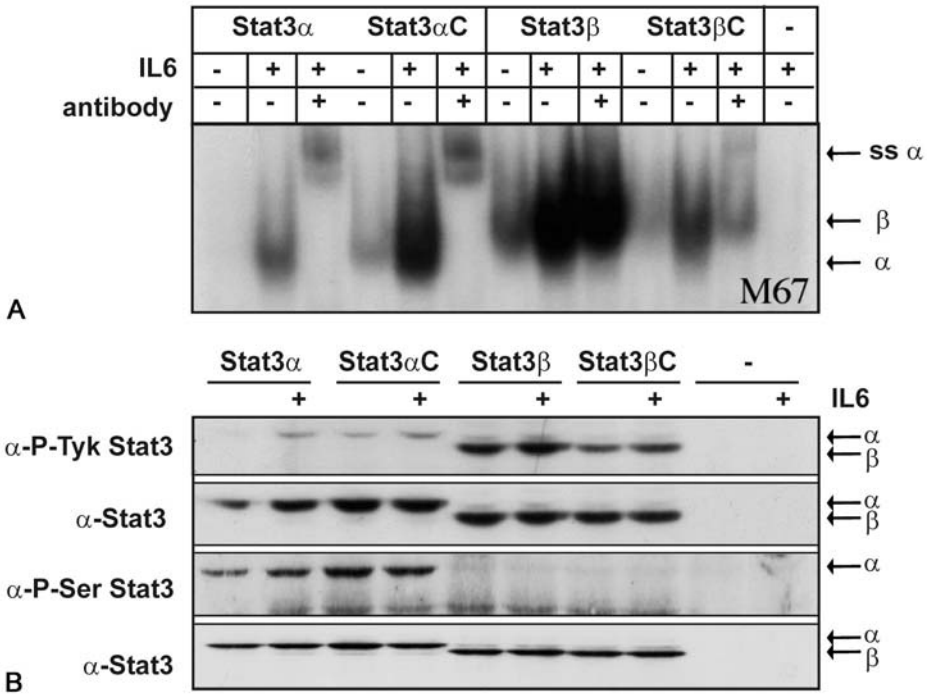

Figure 3. EMSA of 293T cells (A) and Western Blot analysis of Stat3-/- fibroblasts (B) retrovirally transfected with either Stat3alpha, Stat3alphaC, Stat3beta and Stat3betaC. Whole cell extracts were prepared from 293T cells either stimulated with mIL-6 (20 ng/ml) for 30 minutes or cells which were left untreated. Stat3alphaC, Stat3beta and Stat3betaC showed constitutive DNA binding – an effect which was further enhanced upon stimulation with mIL-6. Lack of endogenous Stat3 protein is shown in the last two lanes in panel B.

Stat3betaC (data not shown). It is also worth mentioning that we obtained an infection rate of about 50% using the empty vector alone or 10 to 20% using a Stat5 construct, whereas we only obtained infection rates around 1-2% using the retroviral vectors encoding any version of Stat3 in primary bone marrow cells (Figure 4 and data not shown). The infected bone marrow was subsequently used to transplant lethally irradiated mice that were followed over a fifteen month's period after transplantation. Six weeks after the transplantation, peripheral blood was drawn and analyzed for the presence of GFP^+ cells. Mice that had received a constitutive active mutant of Stat5 showed significant numbers of GFP^+ cells in the periphery (Figure 4B). In contrast, the peripheral blood of the animals transplanted with versions of Stat3 – irrespective of which construct had been used – only possessed low levels of GFP^+ cells (Figure 4B). Mice that had been transplanted with bone marrow after infection with the empty vector or wild type Stat3alpha did not develop any abnormalities up to 15 months of age. At this time point the animals were sacrificed (Figure 4C). In contrast, all mice that had received Stat3alphaC or Stat3beta developed leukemia and/or lymphoma as early as 3 months after transplantation. The animals had severely enlarged spleens, suffered from hepatomegaly and displayed enlarged intestinal lymph nodes (Figure 4D). Some of the animals also had developed a pronounced thymoma.

4.5. Histological analysis reveals highly aggressive T cell lymphoma/T cell leukemia

FACS analysis was performed from six out of twelve animals and revealed that all malignant cells shared the expression of the surface marker Thy1.2. The cells were therefore classified as T lymphoid cells. In addition, in the three mice that had received bone marrow transduced with Stat3alphaC, the infiltrating cells showed expression of CD8, but were negative for CD4. In contrast, in the animals that had received Stat3beta transduced bone marrow the malignant cells were positive for CD4 or double positive for CD4 and CD8 (summarized in Table 1). Surprisingly, we were not able to detect significant GFP expression within the leukemic cells (Figure 4B). We therefore verified the expression of the constitutive active version of Stat3 encoded by the retrovirus by RT-PCR. To do so, cDNA was prepared from leukemic cells from four diseased animals of each group. As depicted in Figure 5A the expression of the retroviral construct was readily detectable in samples derived from the retroviral producers as well as in the samples derived from the diseased animals. Moreover, we unequivocally verified that the leukemic cells were donor-derived and not the consequence of the lethal irradiation of the recipient animals. Analysis of the Y chromosome (we used male donors and female recipient mice) clearly linked the leukemic cells to the donor (Figure 5B). Histological samples of the diseased animals revealed a remarkable picture. All organs investigated were densely

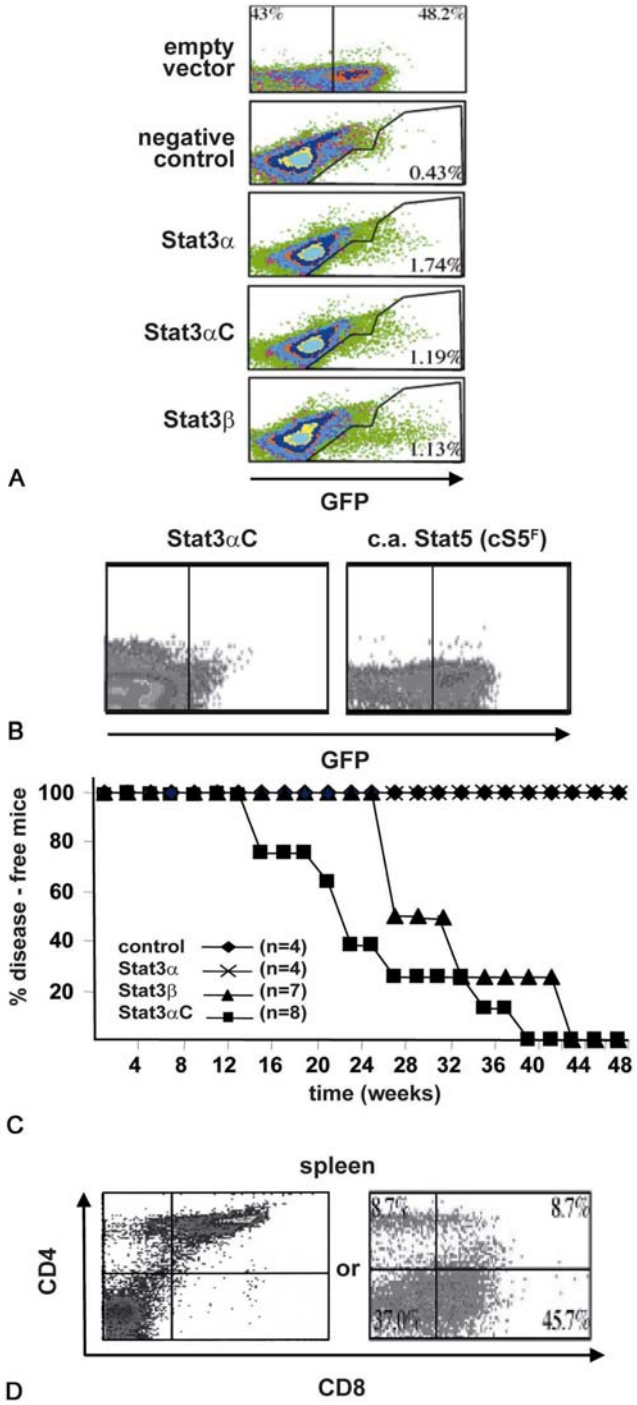

Figure 4. Overexpression of Stat3alphaC or Stat3beta leads to T lymphoid tumors *in vivo*. (A) Donor bone marrow cells were co-cultivated for 48 hours on retroviral producer cell lines in the presence of mIL-3 (20 ng/ml), mIL-6 (50 ng/ml) and mSCF (500 ng/ml). Infection rates of donor bone marrow cells were measured by flow cytometry. (B) Analysis of GFP^+ cells in the peripheral blood four months after transplantation. Peripheral blood from mice that received bone marrow retrovirally transduced with a persistently active Stat5 mutant ($cS5^F$) (45) was analyzed as a control. (C) Kaplan-Meier plot analysis of lethally irradiated C57/Bl6 x Sv/129 F1 mice that received a transplant of donor bone marrow either transduced with Stat3alpha, Stat3alphaC, Stat3beta or the empty vector. (D) Representative photograph of enlarged spleen and intestinal lymph nodes of a terminally diseased mouse. (E) Representative flow cytometric analysis of splenic cells of two terminally diseased mice. Typically, cells were no longer GFP^+, but stained clearly positive for T lymphoid markers (CD4, CD8).

Table 1. Infiltration of T lymphoid cells in liver and spleen of lethally irradiated C57Bl/6 x Sv129 F1 mice transplanted with either Stat3beta or Stat3alphaC transduced bone marrow cells

mouse no.	retroviral construct	$Thy1.2^+CD4^+$		$Thy1.2^+CD8^+$		$Thy1.2^+CD4^+CD8^+$	
		liver	spleen	liver	spleen	liver	spleen
1	Stat3alpha	6.8%	14.4%	6.1%	5.4%	0.2%	0.5%
2	Stat3alpha	5.7%	12.2%	4.8%	6.8%	0%	0.2%
3	Stat3beta	4.8%	4.5%	0.4%	0.3%	46.2%	45.7%
4	Stat3alphaC	2.8%	5.9%	40%	46.7%	0%	0%
5	Stat3alphaC	24.5%	8.6%	28.7%	65.1%	0.5%	0.5%
6	Stat3beta	61.5%	64.4%	0.5%	0.7%	2.6%	5.3%
7	Stat3beta	4.2%	9.6%	5%	5.6%	23.5%	36.7%
8	Stat3alphaC	16.1%	8.7%	23.7%	45.7%	2.5%	8.7%

infiltrated with lymphocytic cells. These included not only the hematopoietic organs such as spleen and lymph nodes, but also the parenchymatous organs like liver, lung, kidney and salivary gland. The malignant cells were even found throughout the pericardium infiltrating the heart muscle (Figure 6). The pattern of the lymphoid infiltrate was most consistent with a highly malignant lymphoma. The appearance of the cells was homogenous; the nuclei had a dense chromatin with relatively prominent nucleoli and a high proliferation rate indicated by high numbers of mitotic figures. The T-lymphoid origin of the malignant cells was further confirmed by anti-CD3 staining that revealed an almost homogenous T cell infiltrate (Figure 7A). The destructive infiltration pattern underscored the malignant potential of the disease. Since Stat3 was reported to suppress Fas expression and to regulate Fas/FasL induced apoptosis in malignant T cells (21), we also analysed Fas and FasL expression. We found that the malignant cells were characterized by the consistent expression of both, Fas and FasL (Figure 7B and 7C and data not shown).

5. DISCUSSION

In this manuscript we demonstrate that Stat3 possesses both, proto-oncogenic as well as tumor suppressing activities depending on the cellular context.

When expressed in primary mouse embryonic fibroblast, Stat3alphaC was capable of efficiently suppressing c-myc induced transformation as well as spontaneous transformation provoked by forced expression of bcl_{xL}. Transformation and tumor formation by rasV12 was not affected. Among the downstream targets of Stat3alphaC that counteract transformation are the AP-1 transcription factor JunB and the cell cycle inhibitor protein $p16^{INK4a}$ (22). JunB homodimerizes to induce its target genes and thereby blocks proliferation and transformation in fibroblasts. JunB is antagonized by heterodimerization with c-Jun. It is attractive to speculate that rasV12 induced transformation escapes Stat3alphaC induced suppression by up-regulation of c-Jun protein.

Our observations differ from the original observation made by Bromberg and colleagues who first defined Stat3alphaC as an oncogene in a single immortalized cell line (4). They found that the single expression of Stat3alphaC sufficed to transform rat fibroblasts and to induce tumor formation in *nu/nu* mice. Differences in the experimental procedures may explain this apparent contradiction; the use of primary mouse embryonic fibroblasts cannot be directly compared with experiments carried out in established and immortalized cell lines that had been maintained in culture for long time and where additional mutations cannot be ruled out. Furthermore, one might also reason that the deletion of p53 - as in our primary cells - might alter cellular responses upon Stat3alphaC activation. A direct interaction between Stat3 and p53 has been reported (23). Recent evidence showed that the deletion of a single gene like the Stat3 target gene SOCS-3 suffices to convert the anti-apoptotic properties of Stat3 into a pro-apoptotic function (24). The deletion of SOCS-3 in MEFs altered the expression and activation levels of Stat3 that as a consequence either induced apoptosis or protected from cytokine-induced apoptosis.

Whereas our study in fibroblasts defined Stat3 as a tumor suppressor, our observations in hematopoietic cells confirmed the general concept that Stat3 is a potent proto-oncogene. Expression of a constitutive active version of Stat3 induced a highly aggressive T cell lymphoma/leukemia upon bone marrow transplantations. The induction of the T cell malignancy required the constitutive activation of Stat3, as wild type Stat3 did not induce disease. This observation supports the concept that a permanent genetic programming of the cells is required to induce the transformed state. Stat3alphaC transduction induced malignant cells with the surface markers CD3 and CD8, whereas Stat3beta was associated with CD4 expression in the malignant cells. In two Stat3beta cases double positive cells (CD4/CD8) were found. Apart from these differences the phenotype of the disease looks superimposable irrespective whether the animals had received Stat3alphaC or Stat3beta transduced bone marrow cells. Another feature of the experiment was puzzling. The initial transduction of freshly isolated bone marrow cells with Stat3 constructs resulted in a significantly lower infection rate compared to controls with the empty vector alone or the infection with construct encoding an oncogenic version of Stat5. We reasoned that hematopoietic cells only tolerate a certain range of Stat3 expression and activation. We also found that v-abl transformed B lymphoid cells did not tolerate the enforced expression of Stat3alphaC (V. Sexl, unpublished observation). The low expression was not a feature of the retroviral constructs, since the identical Stat3 constructs resulted in a significantly elevated Stat3 and GFP expression in other cell types such as fibroblasts. Hematopoietic stem cells depend on Stat3alphaC for self-renewal, the enforced expression of Stat3alphaC had no effect on stem cell function. It is therefore more likely that elevated Stat3 activation is not tolerated at the level of progenitor cells where Stat3 activation might be linked to differentiation and growth inhibition (25, 26). Interestingly,

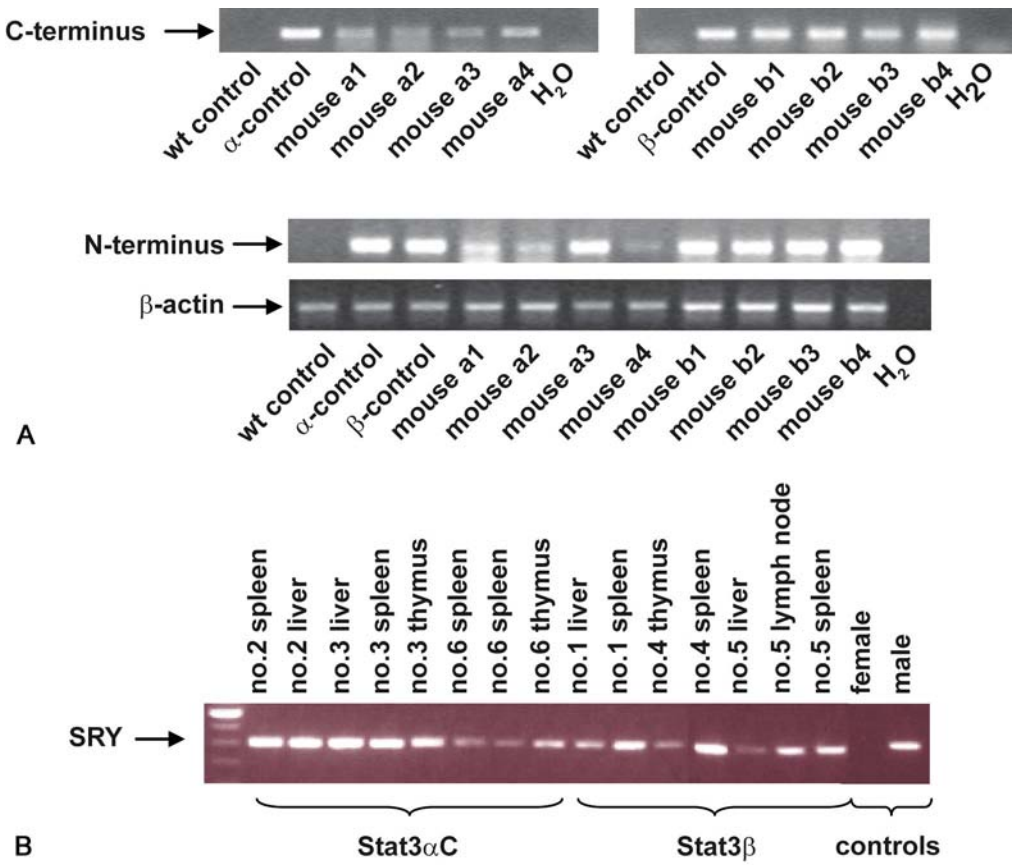

Figure 5. RT-PCR analysis to show retroviral expression in tumor tissues of mice that received bone marrow transduced with either Stat3alphaC or Stat3beta. (A) RNA was isolated and analyzed by RT-PCR for retrovirally inserted Stat3. Detection of Stat3 C- and N-terminus is shown for four Stat3alphaC (mouse a1-a4) and four Stat3beta (mouse b1-b4) recipients. Tissue of a naïve wt mouse (wt control) and Stat3alpha (alpha control) and Stat3beta (beta control) producer cells were used as controls. (B) Male mice served as donors whereas female mice were used as recipients. cDNA from leukemic cells was subjected to SRY specific PCR analysis. Tissues from female and male mice were used as negative or positive controls, respectively.

our observations are in contrast to data obtained by others where the enforced expression of Stat3alphaC in hematopoietic cells did not induce malignancy and Stat3 expression was tolerated by hematopoietic cells (26, 27). We have currently no satisfying explanation for this discrepancy; one reason might be the use of fundamentally different experimental procedures with regard to both, the packaging of the retrovirus as well as the generation and infection of the primary bone marrow cells.

The Stat3 target JunB has been associated with growth inhibition and decreased transformation in B lymphoid cells, whereas it is expressed at elevated levels in T cell malignancies (28). Both, Stat3 and JunB have been demonstrated to enhance NPM-ALK induced tumor formation (6, 29). Ultimatively, the fatal T cell disease induced by transplantation of Stat3 transduced bone marrow is most likely the consequence and result of Stat3 regulating hematopoiesis at various levels.

However, at the time point of fatal disease the malignant cells lacked significant GFP expression although the retroviral insertion and expression within the leukemic cells was unequivocally demonstrated. Overall, the disease can clearly be linked to activated Stat3 proteins, since the forced expression of wild type Stat3 or the empty vector did not result in any tumor development. We have currently no convincing explanation for this phenomenon. Based on the low expression levels of activated Stat3 a significant contribution of Stat3 induced immuno-suppression appears unlikely (12).

One of the most characteristic common features of the malignant cells was their highly aggressive and invasive behavior. The transformed cells did not only infiltrate hematopoietic organs but also lung, liver, salivary glands, and were even found throughout the pericardium infiltrating the myocardial muscle. A key function for Stat3 in T cell infiltration by regulating chemokine secretion and chemokine receptor expression has been demonstrated (30). Moreover, in an *in vivo* model for peritoneal inflammation T cell recruitment, but not B cell recruitment crucially depended on Stat3 activation (30). Apart from chemokine signaling Stat3 regulates the expression of several genes that are involved in wound healing and metastasis (31). In particular, the expression of metallo-proteinases - critical

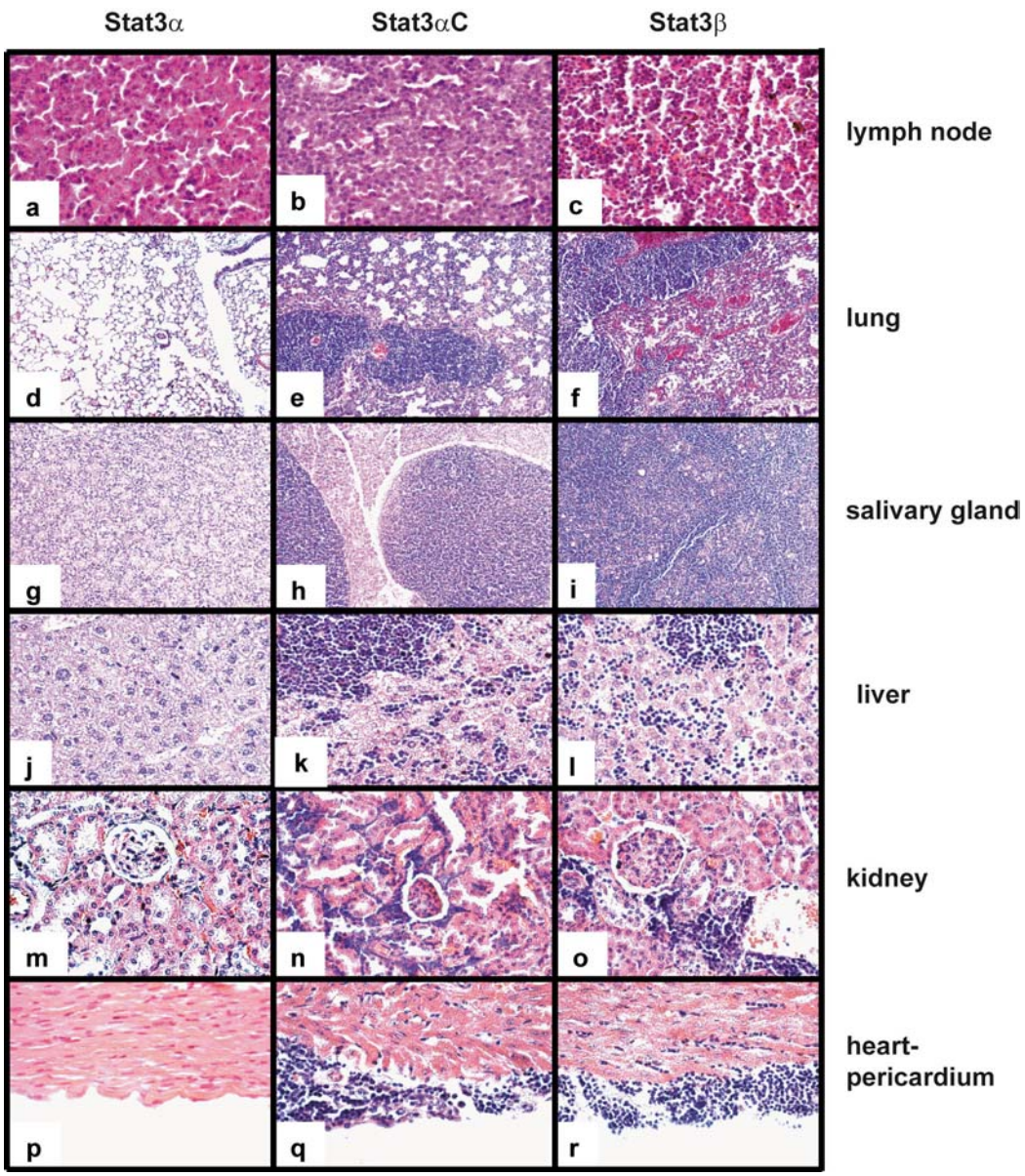

Figure 6. Histopathology analysis after H&E staining from Stat3alpha, Stat3alphaC and Stat3beta retrovirally transduced mice. **a-c:** lymph nodes, 600x magnification; d-f: lung, 100x magnification g-i: salivary gland, 100x magnification; j-l: liver, 400x magnification m-o: kidney, 400x magnification; p-r: heart-pericardium, 400x magnification. Organs of Stat3alpha transduced mice show normal organ architecture without inflammation. Organs of Stat3alphaC and Stat3beta transduced mice show a severe and often homogenous lymphocyte infiltration.

determinants of invasion and metastasis - depend on Stat3 proteins (32-34). Several metalloproteinases are transcriptionally regulated by Stat3. A significant correlation between Stat3-phosphorylation and tissue invasiveness has also been described in human tumors. In gastric, ovarian and colorectal carcinoma as well as cutaneous squamous cell carcinoma a high activation level of Stat3 was associated with a high depth of tumor invasion (35-38). Besides transcriptional effects, Stat3 also directly enhance cell migration by direct interaction with components of the cytoskeleton (39). In ovarian cancer cells phosphorylated Stat3 was found to localize to migrating protrusions (37). Others implicated Stat3 downstream of RhoGTPase induced cell migration or in signaling downstream of integrins (40, 41). Although different mechanisms and signaling pathways were described in all these reports they reached a common conclusion, namely that the activation of Stat3 increased the motility of cells. These properties – enhanced cell migration and increased tissue invasiveness – seem to be mediated by both, Stat3alphaC and Stat3beta. Some of these features are reminiscent of TH17 cells that also need to infiltrate tissues and where Stat3 has recently been described as a key regulator (42-44).

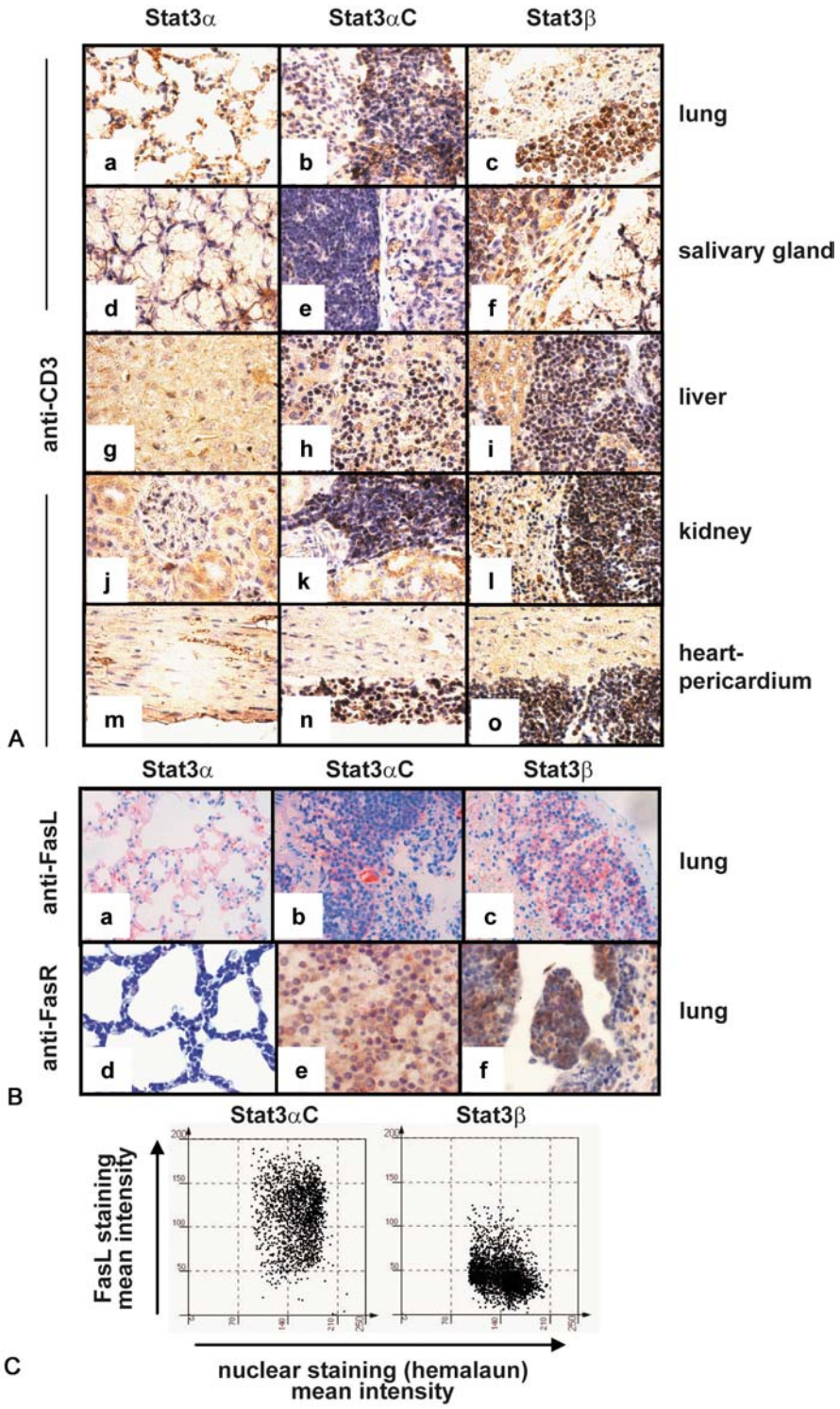

Figure 7. Immunohistochemical T cell marker analysis (anti-CD3), FasR and FasL immunostainings from Stat3alpha, Stat3alphaC and Stat3beta retrovirally transduced mice. (A) 400x magnification a-c: lung d-f: salivary gland g-i: liver j-l: kidney m-o: heart-pericardium. Lymphocytic infiltrates in Stat3alpha transduced mice are almost exclusively composed of T-cells. (B) a+d, normal lung, b+c, anti-FasL immunostaining of lung tissue, d+f anti-FasR immunostaining of lung tissue; 400x magnification. (C) Quantification of immunohistochemical stainings was performed with the HistoQuest analysis software (TissueGnostics, Vienna, Austria) using an average of four fields of view. Pictures were taken with a PixeLINK camera on a Zeiss Imager Z.1 at a magnification of 400x (for details on the quantification method see www.tissuegnostics.com).

Our work elucidates a novel aspect of the biology of Stat3. It defines Stat3 as tumor promoting agent capable of inducing a T cell malignancy. In addition we provide evidence that in some cells activated Stat3 may also suppress tumorigenesis.

5. ACKNOWLEDGEMENTS

Andrea Ecker and Olivia Simma as well as Richard Moriggl, and Veronika Sexl contributed equally to this work. This work was supported by the Austrian Science Foundation (FWF- SFB 28 and grant P19723-B03) and the Austrian genome program GenAu-DRAGON. Olivia Simma received a stipend from The Austrian Academy of Science (OeAW). We thank David E. Levy for the generous gift of $Stat3^{-/-}$ fibroblasts and Michaela Schlederer for excellent technical assistance. We are indebted to Mathias Müller, Ernst Müllner, Boris Kovacic, Robert Eferl, Valeria Poli and Thomas Decker for helpful comments through the course of our work.

6. REFERENCES

1. James E. Darnell Jr: STATs and gene regulation. *Science*, 277: 1630-1635 (1997)

2. Sushil G. Rane and E. Premkumar Reddy: JAKs, STATs and Src kinases in hematopoiesis. *Oncogene*, 21: 3334-3358 (2002)

3. Christian Schindler, David E. Levy, and Thomas Decker: JAK-STAT signaling: from interferons to cytokines. *J Biol Chem*, 282: 20059-20063 (2007)

4. Jacqueline F. Bromberg, Melissa H. Wrzeszczynska, Geeta Devgan, Yanxiang Zhao, Richard G. Pestell, Chris Albanese and James E. Darnell, Jr.: Stat3 as an oncogene. *Cell*, 98: 295-303 (1999)

5. Keith Syson Chan, Shigetoshi Sano, Kaoru Kiguchi, Joanne Anders, Nobuyasu Komazawa, Junji Takeda and John DiGiovanni: Disruption of Stat3 reveals a critical role in both the initiation and the promotion stages of epithelial carcinogenesis. *J Clin Invest*, 114: 720-728 (2004)

6. Roberto Chiarle, William J. Simmons, Honjying Cai, Girish Dhall, Alberto Zamo, Regina Raz, James G. Karras, David E. Levy and Giorgio Inghirami: Stat3 is required for ALK-mediated lymphomagenesis and provides a possible therapeutic target. *Nat Med*, 11: 623-629 (2005)

7. Doris Germain and David A. Frank: Targeting the cytoplasmic and nuclear functions of signal transducers and activators of transcription 3 for cancer therapy. *Clin Cancer Res*, 13: 5665-5669 (2007)

8. Giorgio Inghirami, Roberto Chiarle, William J. Simmons, Roberto Piva, Karni Schlessinger and David E. Levy: New and old functions of STAT3: a pivotal target for individualized treatment of cancer. *Cell Cycle*, 4: 1131-1133 (2005)

9. James Turkson: STAT proteins as novel targets for cancer drug discovery. *Expert Opin Ther Targets*, 8: 409-422 (2004)

10. Toshiyuki Fukada, Masahiko Hibi, Yojiro Yamanaka, Mariko Takahashi-Tezuka, Yoshio Fujitani, Takuya Yamaguchi, Koichi Nakajima and Toshio Hirano: Two signals are necessary for cell proliferation induced by a cytokine receptor gp130: involvement of STAT3 in anti-apoptosis. *Immunity*, 5: 449-460 (1996)

11. Kenneth Leslie, Cynthia Lang, Geeta Devgan, Janeen Azare, Marjan Berishaj, William Gerald, Young Bae Kim, Keren Paz, James E. Darnell, Christopher Albanese, Toshiyuki Sakamaki, Richard Pestell and Jacqueline Bromberg: Cyclin D1 is transcriptionally regulated by and required for transformation by activated signal transducer and activator of transcription 3. *Cancer Res*, 66: 2544-2552 (2006)

12. Hua Yu, Marcin Kortylewski and Drew Pardoll: Crosstalk between cancer and immune cells: role of STAT3 in the tumour microenvironment. *Nat Rev Immunol*, 7: 41-51 (2007)

13. Diego Maritano, Michelle L. Sugrue, Silvia Tininini, Sarah Dewilde, Birgit Strobl, XinPing Fu, Victoria Murray-Tait, Roberto Chiarle and Valeria Poli: The STAT3 isoforms alpha and beta have unique and specific functions. *Nat Immunol*, 5: 401-409 (2004)

14. Andrea Hoelbl, Boris Kovacic, Marc A. Kerenyi, Olivia Simma, Wolfgang Warsch, Yongzhi Cui, Hartmut Beug, Lothar Hennighausen, Richard Moriggl, and Veronika Sexl: Clarifying the role of Stat5 in lymphoid development and Abelson-induced transformation. *Blood*, 107: 4898-4906 (2006)

15. Boris Kovacic, Dagmar Stoiber, Richard Moriggl, Eva Weisz, Rene G. Ott, Rita Kreibich, David E. Levy, Hartmut Beug, Michael Freissmuth and Veronika Sexl: STAT1 acts as a tumor promoter for leukemia development. *Cancer Cell*, 10: 77-87 (2006)

16. Shigeo Saito, Hideyo Ugai, Ken Sawai, Yusuke Yamamoto, Akira Minamihashi, Kahori Kurosaka, Yoshiro Kobayashi, Takehide Murata, Yuichi Obata and Kazunari Yokoyama: Isolation of embryonic stem-like cells from equine blastocysts and their differentiation in vitro. *FEBS Lett*, 531: 389-396 (2002)

17. Emmanuelle Passegue, Erwin F. Wagner and Irving L. Weissman: JunB deficiency leads to a myeloproliferative disorder arising from hematopoietic stem cells. *Cell*, 119: 431-443 (2004)

18. Rene G. Ott, Olivia Simma, Karoline Kollmann, Eva Weisz, Eva-Maria Zebedin, Marina Schorpp-Kistner, Gerwin Heller, Sabine Zochbauer, Erwin F. Wagner, Michael Freissmuth, and Veronika Sexl: JunB is a gatekeeper for B-lymphoid leukemia. *Oncogene*, 26: 4863-4871 (2007)

19. Wei-Chun Chou, David E. Levy, and Chien-Kuo Lee: STAT3 positively regulates an early step in B-cell development. *Blood*, 108: 3005-3011 (2006)

20. Chien-kuo Lee, Regina Raz, Ramon Gimeno, Rachel Gertner, Birte Wistinghausen, Kenichi Takeshita, Ronald A. DePinho and David E. Levy: STAT3 is a negative regulator of granulopoiesis but is not required for G-CSF-dependent differentiation. *Immunity*, 17: 63-72 (2002)

21. P.K. Epling-Burnette, Jin Hong Liu, Robyn Catlett-Falcone, James Turkson, Marc Oshiro, Ravi Kothapalli, Yongxiang Li, Ju-Ming Wang, Hsin-Fang Yang-Yen, James Karras, Richard Jove and Thomas P. Loughran, Jr.: Inhibition of STAT3 signaling leads to apoptosis of leukemic large granular lymphocytes and decreased Mcl-1 expression. *J Clin Invest*, 107: 351-362 (2001)

22. Emmanuelle Passegue and Erwin F. Wagner: JunB suppresses cell proliferation by transcriptional activation of p16(INK4a) expression. *Embo J*, 19: 2969-2979 (2000)

23. Guilian Niu, Kenneth L. Wright, Yihong Ma, Gabriela M. Wright, Mei Huang, Rosalyn Irby, Jon Briggs, James Karras, W. Douglas Cress, Drew Pardoll, Richard Jove, Jiangdong Chen and Hua Yu: Role of Stat3 in regulating p53 expression and function. *Mol Cell Biol*, 25: 7432-7440 (2005)

24. Yang Lu, Satoru Fukuyama, Ryoko Yoshida, Takashi Kobayashi, Kazuko Saeki, Hiroshi Shiraishi, Akihiko Yoshimura, and Giichi Takaesu: Loss of SOCS3 gene expression converts STAT3 function from anti-apoptotic to pro-apoptotic. *J Biol Chem*, 281: 36683-36690 (2006)

25. Ying Guo, Charlie Mantel, Robert A. Hromas, Hal E. Broxmeye: Oct 4 is Critical for Survival/Antiapoptosis of Murine Embryonic Stem Cells Subjected to Stress. Effects Associated with STAT3/Survivin. Stem Cells (2007)

26. Il-Hoan Oh and Connie J. Eaves: Overexpression of a dominant negative form of STAT3 selectively impairs hematopoietic stem cell activity. *Oncogene*, 21: 4778-4787 (2002)

27. Yang-Jo Chung, Bo-Bae Park, Young-Ju Kang, Tae-min Kim, Connie J. Eaves, and Il-Hoan Oh**:** Unique effects of Stat3 on the early phase of hematopoietic stem cell regeneration. *Blood*, 108: 1208-1215 (2006)

28. Agnieszka P. Szremska, Lukas Kenner, Eva Weisz, Rene G. Ott, Emmanuelle Passegue, Michaela Artwohl, Michael Freissmuth, Renate Stoxreiter, Hans-Christian Theussl, Sabina Baumgartner Parzer, Richard Moriggl, Erwin F. Wagner, and Veronika Sexl**.** JunB inhibits proliferation and transformation in B-lymphoid cells. *Blood*, 102: 4159-4165 (2003)

29. Philipp B. Staber, Paul Vesely, Naznin Haq, Rene G. Ott, Kotaro Funato, Isabella Bambach, Claudia Fuchs, Silvia Schauer, Werner Linkesch, Andelko Hrzenjak, Wilhelm G. Dirks, Veronika Sexl, Helmut Bergler, Marshall E. Kadin, David W. Sternberg, Lukas Kenner and Gerald Hoefler: The oncoprotein NPM-ALK of anaplastic large-cell lymphoma induces JUNB transcription via ERK1/2 and JunB translation via mTOR signaling. *Blood*, 110: 3374-3383 (2007)

30. Rachel M. McLoughlin, Brendan J. Jenkins, Dianne Grail, Anwen S. Williams, Ceri A. Fielding, Clare R. Parker, Matthias Ernst, Nicholas Topley and Simon A. Jones: IL-6 trans-signaling via STAT3 directs T cell infiltration in acute inflammation. *Proc Natl Acad Sci U S A*, 102: 9589-9594 (2005)

31. Daniel J. Dauer, Bernadette Ferraro, Lanxi Song, Bin Yu, Linda Mora, Ralf Buettner, Steve Enkemann, Richard Jove and Eric B Haura: Stat3 regulates genes common to both wound healing and cancer. *Oncogene*, 24: 3397-3408 (2005)

32. Svetlana A. Tsareva, Richard Moriggl, Florian M. Corvinus, Bernd Wiederanders, Alexander Schütz, Boris Kovacic and Karlheinz Friedrich: Signal transducer and activator of transcription 3 activation promotes invasive growth of colon carcinomas through matrix metalloproteinase induction. *Neoplasia*, 9: 279-291 (2007)

33. Tong-xin Xie, Daoyan Wei, Mingguang Liu, Allen C Gao, Francis Ali-Osman, Raymond Sawaya and Suyun Huang: Stat3 activation regulates the expression of matrix metalloproteinase-2 and tumor invasion and metastasis. *Oncogene*, 23: 3550-3560 (2004)

34. Masayuki Itoh, Tomomi Murata, Toshiyasu Suzuki, Masahiro Shindoh, Kiyokazu Nakajima, Katsumi Imai, and Kazuo Yoshida: Requirement of STAT3 activation for maximal collagenase-1 (MMP-1) induction by epidermal growth factor and malignant characteristics in T24 bladder cancer cells. *Oncogene*, 25*:* 1195-1204 (2006)

35. Takafumi Kusaba, Toshiyuki Nakayama, Kazuyuki Yamazumi, Yuichi Yakata, Ayumi Yoshizaki, Takeshi Nagayasu, and Ichiro Sekine: Expression of p-STAT3 in human colorectal adenocarcinoma and adenoma; correlation with clinicopathological factors. *J Clin Pathol*, 58: 833-838 (2005)

36. Cai Suiqing, Zheng Min and Chen Lirong: Overexpression of phosphorylated-STAT3 correlated with the invasion and metastasis of cutaneous squamous cell carcinoma. *J Dermatol*, 32: 354-360 (2005)

37. Debra L. Silver, Honami Naora, Jinsong Liu, Wenjun Cheng and Denise J. Montell: Activated signal transducer and activator of transcription (STAT) 3: localization in focal adhesions and function in ovarian cancer cell motility. *Cancer Res*, 64: 3550-3558 (2004)

38. Yuichi Yakata, Toshiyuki Nakayama, Ayumi Yoshizaki, Takafumi Kusaba, Kenichiro Inoue, Ichiro Sekine: Expression of p-STAT3 in human gastric

carcinoma: significant correlation in tumour invasion and prognosis. *Int J Oncol*, 30: 437-442 (2007)

39. Dominic Chi Hiung Ng, Bao Hong Lin, Cheh Peng Lim, Guochang Huang, Tong Zhang, Valeria Poli and Xinmin Cao: Stat3 regulates microtubules by antagonizing the depolymerization activity of stathmin. *J Cell Biol*, 172: 245-257 (2006)

40. Janeen Azare, Kenneth Leslie, Hikmat Al-Ahmadie, William Gerald, Paul H. Weinreb, Shelia M. Violette and Jacqueline Bromberg: Constitutively activated Stat3 induces tumorigenesis and enhances cell motility of prostate epithelial cells through integrin beta 6. *Mol Cell Biol*, 27: 4444-4453 (2007)

41. Marcella Debidda, Lei Wang, Heesuk Zang, Valeria Poli, and Yi Zheng: A role of STAT3 in Rho GTPase-regulated cell migration and proliferation. *J Biol Chem*, 280: 17275-17285 (2005)

42. Xuexian O. Yang, Athanasia D. Panopoulos, Roza Nurieva, Seon Hee Chang, Demin Wang, Stephanie S. Watowich and Chen Dong: STAT3 regulates cytokine-mediated generation of inflammatory helper T cells. *J Biol Chem*, 282: 9358-9363 (2007)

43. Roza Nurieva, Xuexian O. Yang, Gustavo Martinez, Yongliang Zhang, Athanasia D. Panopoulos, Li Ma, Kimberly Schluns, Qiang Tian, Stephanie S. Watowich, Anton M. Jetten and Chen Dong: Essential autocrine regulation by IL-21 in the generation of inflammatory T cells. *Nature*, 448: 480-483 (2007)

44. Liang Zhou, Ivaylo I. Ivanov, Rosanne Spolski, Roy Min, Kevin Shenderov, Takeshi Egawa, David E. Levy, Warren J. Leonard and Dan R. Littman: IL-6 programs T(H)-17 cell differentiation by promoting sequential engagement of the IL-21 and IL-23 pathways. *Nat Immuno*l, *8:* 967-974 (2007)

45. Richard Moriggl, Veronika Sexl, Lukas Kenner, Christopher Duntsch, Katharina Stangl, Sebastien Gingras, Angelika Hoffmeyer, Anton Bauer, Roland Piekorz, Demin Wang, Kevin D. Bunting, Erwin F. Wagner, Karoline Sonneck, Peter Valent, James N. Ihle and Hartmut Beug: Stat5 tetramer formation is associated with leukemogenesis. *Cancer Cel*l, 7*:* 87-99 (2005)

Abbrevations: Stat: Signal transducers and activators of transcription, MEFs: mouse embryonic fibroblasts

Key Words: Stat3, p53, c-myc, rasV12, Cytokine Signaling, Leukemia, Bone Marrow Transplantation, Tumor Suppressor, Tumor Promoter

Send correspondence to: Veronika Sexl, Medical University of Vienna, Centre of Biomolecular Medicine and Pharmacology, Waehringerstrasse 13A, A-1090 Vienna, Austria, Tel: 0043-1-4277-64137, Fax: 0043-1-4277-9641, E-mail: veronika.sexl@meduniwien.ac.at